Journal of Environmental Chemical Engineering 13 (2025) 115425

Contents lists available at ScienceDirect

Journal of Environmental Chemical Engineering

journal homepage: www.elsevier.com/locate/jece

Exploring optical properties and radiation transfer in a mixed culture of purple phototrophic bacteria grown in a flat-plate photobioreactor via combined experimental and modelling approach

Ali Amini [a], Elisa Porciatti [a], Alessandro Minotto [b], Álvaro Tolosana Moranchel [c], Adele Sassella [b], Roberto Canziani [a], Andrea Turolla [a,*]

[a] Department of Civil and Environmental Engineering (DICA), Politecnico di Milano, Piazza Leonardo da Vinci 32, Milan 20133, Italy
[b] Department of Materials Science, University of Milano-Bicocca, via Cozzi 55, Milan 20125, Italy
[c] Grupo de Energía y Química Sostenibles, Instituto de Catálisis y Petroleoquímica, CSIC. Marie Curie 2, Madrid 28049, Spain

ARTICLE INFO

Keywords:
Purple phototrophic bacteria
Photobioreactor
Radiation transfer
Optical properties
Local volumetric rate of photon absorption
Computational Fluid Dynamics

ABSTRACT

The optimization of radiation transfer in a mixed culture of purple phototrophic bacteria (PPB) inside a photobioreactor (PBR) is crucial for maximizing growth efficiency and resource recovery. In this study, the optical behavior of PPB mixed cultures was characterized from 300 nm to 1100 nm at different incident light intensities of 10 W•m^{-2}, 20 W•m^{-2}, 40 W•m^{-2}, and 60 W•m^{-2}, and at different biomass concentrations. Experimental data were processed via empirical and Monte Carlo methods to determine the optical properties. Various models, namely the Beer-Lambert law, the two-flux approximation model, and computational fluid dynamics (CFD) simulations, were then applied to describe the radiation transfer inside the PBR. Among the most relevant results, the adaptation of absorption peaks as a function of light intensity was observed. Moreover, the scattering effect was found to be non-negligible, characterized by a strong non-isotropic nature. Although the scattering effect was significant, the results showed that the Beer-Lambert law can effectively describe the light attenuation profiles, resulting in irrelevant errors in calculating the light intensity at each layer of the PBR compared to the two-flux approximation model and CFD simulations, in turn characterized by higher computational costs. However, simpler models could lead to higher values for the local volumetric rate of photon absorption along different layers, especially at lower concentrations. Finally, the results suggest that flat-plate PBRs illuminated from both sides can be an effective solution for PPB systems compared to raceway ponds, mainly due to the enhanced two-sided short-path light penetration.

1. Introduction

The high potential of purple phototrophic bacteria (PPB) to be applied in biotechnologies for simultaneously treating waste streams and recovering valuable resources such as carotenoids, single-cell proteins, polyhydroxyalkanoates, and fertilizers has been recognized for many years [1–3]. Due to their ability to exploit light as a source of energy, PPB biomass yields can approach unity (in terms of COD removed), maximizing the recovery potential [4]. PPB collect light in the visible spectrum (400 – 600 nm) through a variety of carotenoids [5] and in the near-infrared spectrum (NIR; primarily around 800–900 nm) through bacteriochlorophylls [6].

So far, PPB have commonly been cultivated in photobioreactors (PBRs) exposed to artificial light [4]. To enhance microbial kinetics in PBRs, the optimization of radiation transfer is crucial: light must be delivered at the proper wavelength, intensity, and duration. High light intensities can cause photooxidation and photoinhibition, while low values can hinder growth [7]. In addition, for process design and operation, the light intensity distribution in PBRs is of paramount importance. Besides the optical characteristics of treated wastewater, the attenuation profile of light intensity is determined by the suspension of photosynthetic microorganisms, which also depends on their concentration [8]. In fact, light intensity is reduced along the irradiation path due to the occurrence of optical phenomena (absorption and scattering) determined by the constituents of the aqueous medium and the PPB cells [8,9]. Therefore, in view of effective process application, it

* Corresponding author.
E-mail address: andrea.turolla@polimi.it (A. Turolla).

https://doi.org/10.1016/j.jece.2025.115425
Received 11 September 2024; Received in revised form 13 November 2024; Accepted 11 January 2025
Available online 18 January 2025

is essential to properly assess the radiation transfer within PBRs, which is usually done by mathematical modelling tools [10].

To date, most modelling efforts related to radiation transfer in phototrophic engineered systems have been performed on microalgae [11], with such research demonstrating that it is the primary factor that restricts the productivity of PBRs [12]. While these investigations can be considered as the starting point for the development of PPB-based biotechnologies, their results cannot be directly extrapolated as the physical and biochemical processes of microalgae and PPB differ significantly, and their adaptation is needed [10,13].

In the view of modelling photo(bio)chemical systems, the radiative transfer equation (RTE) is typically used to describe the radiative fields in a participating medium [14]. To solve the RTE in a photo(bio) chemical reactor, the estimation of optical properties such as the absorption coefficient, scattering coefficient, and scattering phase function is required [15]. This information is further utilized in deterministic or stochastic models to compute the radiation intensity and the local volumetric rate of photon absorption (LVRPA), the latter being the number of photons absorbed in a unit of volume medium and in a unit of time. Such variables are the critical parameters relating the radiation distribution to the local reaction kinetics [16].

The RTE can be solved using a variety of different modelling approaches, such as the Beer-Lambert law, the two-flux approximation model, and the discrete ordinate method (DOM) [17]. Among the various methods, the Beer-Lambert law is the most widespread for modelling microalgae PBR [18,19]. It accounts for one-directional light attenuation through the culture, and irradiance at any point inside the PBR can be computed as a function of incident light intensity, optical path, and biomass concentration [11]. However, the most significant drawback of the Beer-Lambert law is that it does not account for the scattering effect, which has been determined to be non-negligible for algal biomass concentrations above 100 mg•L^{-1} dry weight [20]. In such cases, instead of using the Beer-Lambert law, which aggregates both absorption by pigments and light scattering by cells, a two-parameter model is required [21]. In particular, the two-flux approximation model can be used as a method to account for both light absorption and scattering [12]. More specifically, the two-flux approximation model is derived from the assumptions of Schuster [22], and many authors have utilized this model to compute the irradiance field in PBRs due to its strong predictability for both flat-plate [23] and tubular PBRs [13]. In addition, more precise models have been applied to simulate the distribution of light inside PBRs. For instance, the Monte Carlo method has been employed because of its accuracy and simple application [24]. On the other hand, computational fluid dynamics (CFD) has emerged as an accurate method for determining the distribution of radiation intensity in complex geometries [25], although at high computational costs.

Currently, the modelling of the radiation transfer within PBRs applying PPB-based biotechnologies remains relatively understudied, as well as the determination of the related parameters describing the relevant optical properties, and only a few studies have been conducted, leaving a noticeable gap in the understanding of the phenomena that impacts radiation transfer. Although the optical characteristics of PPB mixed cultures have yet to be investigated, Berberoglu and Pilon [29] conducted experimental measurements on the optical properties in a hydrogen-producing PPB pure culture [26]. The results showed that scattering was not negligible, and the scattering phase function demonstrated a pronounced peak in the forward direction. These outcomes suggest that it is important to accurately describe the optical behavior to predict the light attenuation inside PBRs. Then, Capson-Tojo et al. [10] utilized different models to represent light attenuation in PPB PBRs. In this case, the optical characteristics of PPB mixed cultures were not experimentally measured but determined through modelling regression. The results showed that the term accounting for light scattering had minimal effect on light attenuation, with a value of approximately zero.

In the present research work, a combined experimental and modelling approach has been developed to investigate the radiation transfer in flat-plate PBRs for PPB mixed cultures to refine the observations found in the literature, trying to elucidate the missing elements (such as the importance of scattering in PPB systems). First, the optical behaviour of PPB mixed cultures grown on acetate at the laboratory scale was determined from 300 nm to 1100 nm at different incident light intensities ranging from 10 W•m^{-2} to 60 W•m^{-2} and different PPB concentrations (40 mgTSS•L^{-1} – 320 mgTSS•L^{-1}). Experimental data were then processed via empirical and Monte Carlo methods to determine the optical properties, as the optical behaviour of PPB mixed cultures had not been previously studied, to the best of the authors' knowledge. Then, various existing models, namely the Beer-Lambert law, the two-flux approximation model, and CFD simulations, were applied and compared to describe the radiation transfer inside the PBR. Finally, the influence of the most relevant operating conditions (PPB concentration and light intensity) on PBR performance was assessed with the aim of identifying guidelines for optimal system design and operation.

2. Material and methods

2.1. PPB enrichment

A mixed culture of PPB was enriched from an environmental sample collected from a pond in a peri-urban wetland in the Milan area (Northern Italy). Briefly, PPB enrichment was carried out using a 5.6-L cylindrical glass reactor fed with modified Ormerod medium [26], in which biotin, ammonium sulfate, and malic acid were substituted with yeast extract (0.015 mg•L^{-1}), ammonium chloride (150 mgN•L^{-1}), and sodium acetate (1500 mgCOD•L^{-1}), respectively. To avoid and minimize the production of hydrogen within the enrichment PBR, the ratio between COD and N was kept around 10, and the pH was adjusted to 7. The PPB enrichment was performed under anaerobic conditions at 30 ± 1 °C, illuminated with a monochromatic LED strip (Waveform Lighting) at a wavelength of 850 nm attached to the external surface of the enrichment PBR. An opaque box was used to cover the enrichment PBR to avoid the penetration of ambient light, and homogeneous mixing conditions within the PBR were ensured by a magnetic stirrer. After one week, when the appearance of a marked purple color was observed, 1/3 of the volume was decanted and replenished with fresh synthetic medium. The process continued until a deep purple culture was generated, which was used as inoculum for the batch experiments.

2.2. Experimental setup for batch growth

A lab-scale irradiation setup (Figure S1) was constructed to investigate the impact of four different incident light intensities (10 W•m^{-2}, 20 W•m^{-2}, 40 W•m^{-2}, and 60 W•m^{-2}) on a mixed culture of PPB at controlled temperature (30 ± 2 °C) and pH (7 ± 0.1). It is worth mentioning that on clear days at sea level, solar irradiance can peak around 1000 W•m^{-2}, with about 28 % in the near-infrared range [27]. Although the intensities used in this study are lower, they are realistic due to natural sunlight reduction. Atmospheric scattering can decrease direct and diffuse light by 17 %, with additional cuts up to 30 % based on latitude. Cloud cover may further reduce irradiance by 65 %, and culture orientation relative to the sun can lower it by another 50 % [28]. Thus, PBRs in real conditions often receive much less light than the theoretical maximum. All experiments were conducted in triplicate in an opaque box to prevent interference from other light sources. The setup included a control system to adjust the light intensities and to keep the temperature constant. Two wooden panels were mounted vertically close to the internal walls of the box and equipped with 12 LED strips each (Waveform Lighting), emitting a uniform monochromatic (850 nm) radiation field towards the center of the box from each vertical panel. To enable parallel testing at different intensities, black cardboard was inserted between panels to create two distinct radiation zones. Six flat flasks

made of transparent polystyrene, each with a volume of 316.5 mL, a surface area of 75 cm^2, a flask thickness of 3.3 cm, and a wall thickness of 1.5 mm, were used. The flasks were capped to maintain an anaerobic environment, and a multi-magnetic stirrer provided continuous and homogeneous mixing during the experiments. The incident light intensity on the surface of the flasks was measured by a calibrated radiometer (ILT 1400, International Light).

2.3. Estimation of optical properties

2.3.1. Sample preparation

The content of flasks for PPB batch growth was collected and centrifuged for 20 min at 4000 rpm (IEC CL 10 centrifuge, Thermo Scientific). After discarding the supernatant, the biomass was washed and then suspended in a phosphate buffer saline (PBS) solution, providing a non-absorbing and non-scattering medium [29]. The composition of the PBS solution was 8 $g\bullet L^{-1}$ NaCl, 0.2 $g\bullet L^{-1}$ KCl, 0.61 $g\bullet L^{-1}$ Na_2HPO_4, and 0.2 $g\bullet L^{-1}$ KH_2PO_4. The pH of the PBS solution was adjusted to 7 using HCl 3 M. Then, different PPB concentrations, ranging from 40 $mgTSS\bullet L^{-1}$ to 1500 $mgTSS\bullet L^{-1}$, were prepared by dilution using the PBS solution. The higher biomass concentrations up to 1500 $mgTSS\bullet L^{-1}$ were obtained following the methodology described by Capson-Tojo et al. [10]. The total suspended solids (TSS) content was determined via a standard curve based on the optical density (OD_{660}) at 660 nm (reported in Eq. 1) by diluting the PPB batch cultures at the stationary phase. The TSS content was measured according to Standard Methods [30] during the preparation of the standard curve, while the OD_{660} was measured by a spectrophotometer (Hach-Lange, model: DR6000) using 1-cm pathlength glass cuvettes (Hellma Analytics).

$$TSS = 459.22 * OD_{660};\ R^2 = 0.9976 \quad (1)$$

2.3.2. Optical measurements

Sample transmittance (T) was characterized between 300 nm and 1100 nm with a spectrophotometer (Hach-Lange, model: DR6000), using 1-cm pathlength glass cuvettes (Hellma Analytics). Sample diffuse transmittance (%T) and diffuse reflectance (%R) were measured according to the configurations shown in Fig. 1, with a spectrophotometer equipped with a 15-cm-diameter integrating sphere (Lambda 900 UV/VIS/NIR, Perkin Elmer). A 2-mm pathlength quartz cuvette (Hellma Analytics) was used as a sample holder, and the measurements were performed for wavelengths ranging from 300 nm to 1100 nm.

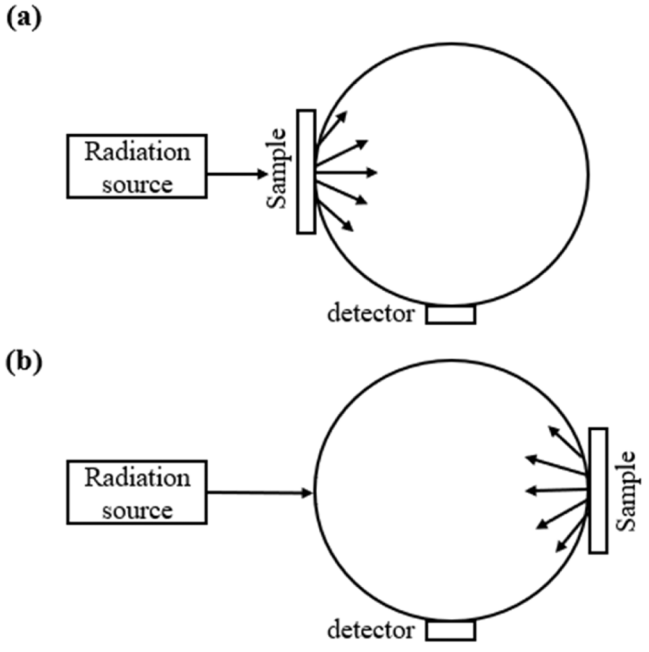

Fig. 1. (a) The experimental setup for diffuse transmittance and (b) diffuse reflectance measurements.

2.3.3. Data processing

Two approaches were used for the measured data. The first approach used in this study is based on the empirical method described by Berberoglu and Pilon [29]. Eqs. 2 – 4 were utilized to determine the extinction coefficient (β_λ), absorption coefficient (κ_λ), and scattering coefficient (σ_λ) for each sample and wavelength with their specific values, respectively. To address the impact of cuvette-based reflection and refraction, measurements were conducted relative to the transmission spectrum of the cuvette containing only PBS.

$$\beta_\lambda = -\frac{1}{t}\ln\left(\frac{T_{\lambda,X}}{T_{\lambda,PBS}}\right) \quad , \quad \beta_\lambda^* = \frac{\beta_\lambda}{X} \quad (2)$$

$$\kappa_\lambda = -\frac{1}{t}\ln\left(\frac{\%T_{\lambda,X}}{\%T_{\lambda,PBS}}\right) \quad , \quad \kappa_\lambda^* = \frac{\kappa_\lambda}{X} \quad (3)$$

$$\sigma_\lambda = \beta_\lambda - \kappa_\lambda \quad , \quad \sigma_\lambda^* = \frac{\sigma_\lambda}{X} \quad (4)$$

Where t corresponds to the thickness of the cuvette used for the measurements, i.e., 1 cm for T and 0.2 cm for %T, $T_{\lambda,PBS}$ and $\%T_{\lambda,PBS}$ are the transmittance and diffuse transmittance of PBS alone in the cuvette, and $T_{\lambda,X}$ and $\%T_{\lambda,X}$ are the transmittance and diffuse transmittance of the PPB suspension with a specific concentration *X*.

The second approach employed in this study for determining the optical properties was based on the Monte Carlo method (MCM), which solves a one-dimensional, one-directional radiation transport model, following the methodology reported previously [31]. With this approach, it was possible to obtain β_λ, κ_λ and σ_λ, and the asymmetry factor (g_λ). The asymmetry factor was determined by averaging the values obtained in MCM for samples with different PPB concentrations. Having defined the asymmetry factor, it is possible to use it for the phase function that accounts for scattering in CFD simulations, which is essential for describing non-isotropic situations. In this work, the Henyey and Greenstein (HG) phase function was used.

2.4. Radiation transfer modelling

As the first approach to describe the light distribution within the PBRs, the Beer-Lambert law, as the simplest model, was applied according to Eq. 5:

$$I_z = I_0 \cdot \exp(-\varepsilon \cdot X \cdot z) \quad (5)$$

Where I_z ($W\bullet m^{-2}$) is the light intensity of the beam after a path length of z (cm) through the medium, I_0 ($W\bullet m^{-2}$) is the incident light intensity at the surface of the PBR, ε ($m^2\bullet g^{-1}$) is the mass extinction coefficient, and X ($g\bullet m^{-3}$) is the biomass concentration.

Subsequently, to consider both light absorption and scattering by cells, a two-flux approximation model was employed to provide an analytical solution. Since the lab-scale PBR was designed to have incident radiation only on one side of each reactor, Eqs. 6, 7, and 8 were applied in all four experiments at different light intensities to obtain the specific absorption coefficient (E_a) and the specific scattering coefficient (E_s) [23]. These values were estimated by using the Curve Fitting Toolbox in MATLAB.

$$\frac{I_z}{I_0} = \frac{4a_1}{(1+a_1)^2 e^{a_2} - (1-a_1)^2 e^{-a_2}} \quad (6)$$

$$a_1 = \sqrt{\frac{E_a}{E_a + E_s}} \quad (7)$$

$$a_2 = (E_a + E_s)\cdot a_1 \cdot X \cdot z \quad (8)$$

Where E_a ($m^2 \bullet g^{-1}$) is the specific absorption coefficient, and E_s ($m^2 \bullet g^{-1}$) is the specific scattering coefficient.

Once the light attenuation was estimated by assuming a well-mixed condition, the average light intensity along the reactor that each bacterium could receive was obtained according to Eq. 9 [19]:

$$I_{average} = \frac{1}{L}\int_0^L I(z)\cdot d_z \quad (9)$$

Where $I_{average}$ ($W \bullet m^{-2}$) is the average light intensity, L (m) is the total light path length, I (z) ($W \bullet m^{-2}$) is the light intensity at each length step, and dz (m) is the different length steps.

Finally, CFD simulations were used as the most accurate approach for modelling the radiation transfer in this study. A two-dimensional geometry design was created using Ansys SpaceClaim (version 2021 R2), which includes the flask (90 mm × 36 mm) with a thickness of 1.5 mm and the PPB culture inside the flask (87 mm × 33 mm). This setup is surrounded by a 100 mm × 46 mm space (air), through which light emitted from LEDs enters via an inlet radiation boundary (see Figure S2 (a) in Supplementary Material). Following the geometry generation, quadrilateral meshes were created using Ansys Meshing (version 2021 R2) to obtain a precise distribution of light within the PBR. To ensure adequate grid resolution, a grid independence analysis was conducted using two structured grids consisting of 18,400 and 51,380 quadrilateral elements. Simulation results indicated that the difference between the two grids was less than 1 %. Based on these findings, it was concluded that the grid with 18,400 elements adequately represents the case under study. However, the grid with 51,380 elements (see Figure S2 (b) in Supplementary Material) was chosen for all simulations to provide enhanced resolution. The basic governing conservation equation for describing radiation transfer is the RTE. The basic RTE at position *r*, in the direction *s*, can be written as [32]:

$$\frac{dI_\lambda(r,s)}{ds} = \kappa_\lambda \cdot I_\lambda - (\kappa_\lambda + \sigma_\lambda)\cdot I_\lambda(r,s) + \frac{\sigma_{\lambda,s}}{4\pi}\int_0^{4\pi} I_\lambda(r,s')\cdot\phi_\lambda(s,s')d\Omega' \quad (10)$$

Where the phase function Φ (s, s') accounts for scattering from the direction s' to the direction s and determines the fraction of in-scattering radiation.

The left side of Eq. 10 shows the change in radiation intensity along a direction. On the right side, the first term is positive and represents black-body radiation. The second term is negative, indicating attenuation from absorption and scattering, which are key aspects of this study. Finally, the last positive term accounts for in-scattering through the phase function. Since the DO model has emerged as one of the best solutions for solving the RTE [32], it was used to simulate the light distribution within the lab-scale PBR. The DO model effectively solves the RTE by using a finite number of discrete solid angles, defined by appropriately setting the parameters for angular discretization, for which a value of 5 was identified as appropriate. This choice was based on preliminary simulations that tested various levels of angular discretization. A setting of 5 provided a balanced compromise between computational cost and accuracy, as increasing the discretization beyond this value did not yield significant improvements in accuracy but resulted in higher computational demands. Moreover, the radiative output of the LEDs was characterized by non-gray radiation, with wavelengths falling within the range of 845 nm to 855 nm. A semi-transparent boundary condition type was assigned for all the reactor walls and the inlet radiation boundary, while an opaque boundary condition type was set for the other walls, with an internal emissivity and diffuse fraction equal to one. Direct irradiation was applied to the radiation boundary, and it was calibrated to have the same irradiance on the surface of the flask. For describing the distribution of light in the PBR, the optical properties obtained in this study for different PPB concentrations grown under different incident light intensities were utilized as initial conditions. Moreover, a linear anisotropic scattering phase function and refractive index of 1.3 were assigned for the simulations. To achieve accurate solutions, the maximum achievable number of iterations and convergence tolerance were fixed at 250 and 10^{-6}, respectively.

After obtaining the light distribution within the PBRs, it is possible to determine the LVRPA expressed in $Einstein \bullet m^{-3} \bullet s^{-1}$. For monochromatic light intensity at 850 nm, it can be calculated according to Eq. 11:

$$LVRPA = I(z)\cdot\lambda\cdot 0.836\cdot 10^{-8}\cdot A \quad (11)$$

Where λ (nm) is the wavelength equal to 850 and A (m^{-1}) is the absorbance at 850 nm.

3. Results and discussion

3.1. Characterization of the PPB mixed culture

The process of enriching PPB using the modified Ormerod medium consistently resulted in a color change within approximately a week. By replacing one-third of the enrichment reactor with fresh synthetic medium on a weekly basis, a remarkable intensification of color density was observed, until reaching a stationary situation (1.2 $gTSS \bullet L^{-1}$) in about 2 weeks. Upon analysis of the samples taken, distinctive absorption peaks emerged around the wavelength range of 400 nm – 550 nm related to the carotenoid content responsible for the change in color. Furthermore, peaks at 590 nm, 805 nm, and 865 nm indicated the presence of PPB bacteriochlorophylls. These peaks have been observed for batch experiments under different incident light intensities applied.

3.2. Determination of optical properties

The extinction, absorption, and scattering coefficients were determined for different PPB concentrations ranging from 40 $mgTSS \bullet L^{-1}$ to 320 $mgTSS \bullet L^{-1}$ by the two approaches described in Section 2.3.3. Subsequently, these coefficients were normalized based on the corresponding concentrations, obtaining the specific extinction, absorption, and scattering coefficients as defined previously. Fig. 2(a) – (f) show the results obtained from the sample with different PPB concentrations for incident light intensity of 10 $W \bullet m^{-2}$ over the spectral range from 300 nm to 1100 nm.

As shown in Fig. 2, the optical properties obtained by the two procedures were roughly equal over the entire spectral range from 300 nm to 1100 nm. This similarity was consistent for all incident light intensities considered in this study, as shown in Supplementary Material (Figures S3 – S5). As can be observed, there are two absorption peaks in the NIR region due to the presence of PPB bacteriochlorophylls, whereas peaks in the visible range can be attributed to the presence of carotenoids, being such results in agreement with literature [33–35]. As expected, an increase in absorption and scattering coefficients was noticed with increasing the biomass concentrations (Fig. 2(c) and (e)). Upon normalizing these coefficients with their corresponding concentrations, the specific extinction, absorption, and scattering coefficients were determined, aligning closely along a single line. This shows the independence of specific coefficients from PPB concentration, as demonstrated in Fig. 2(b), (d), and (f). It should be noted that for higher concentrations of 700 $mgTSS \bullet L^{-1}$, 1000 $mgTSS \bullet L^{-1}$, and 1500 $mgTSS \bullet L^{-1}$ (data not shown), the results aligned with the trend observed at lower concentrations. However, these higher concentrations posed a challenge due to the settling of biomass during the measurement process. This settling phenomenon caused inaccuracies, impeding the precise determination of optical properties.

To better understand how various incident light intensities impact the optical properties of PPB, it was essential to compare different

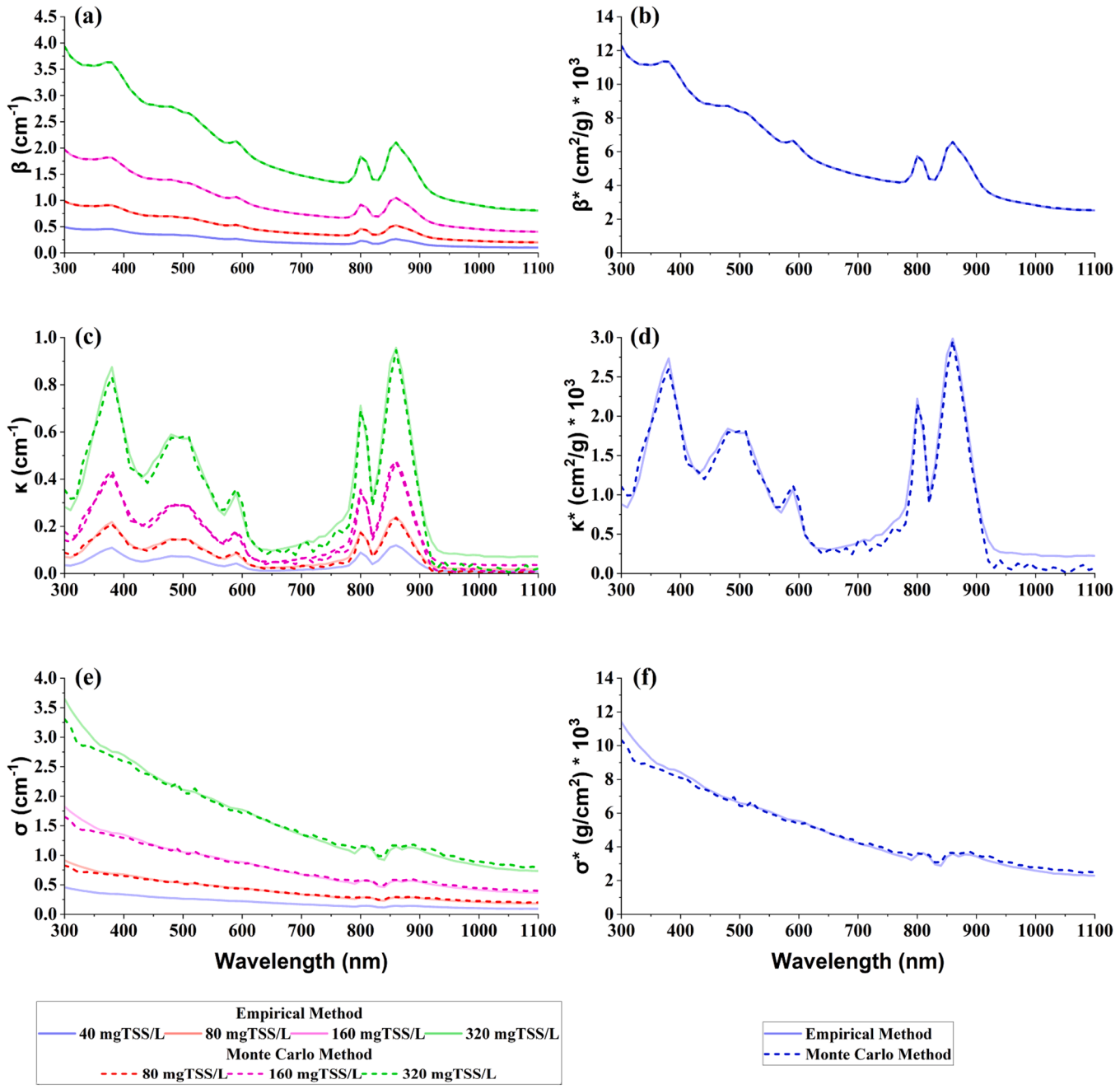

Fig. 2. Spectral (a) extinction, (c) absorption, and (e) scattering coefficients, and the corresponding specific (b) extinction, (d) absorption, and (f) scattering coefficients measured at different PPB concentrations from 300 nm to 1100 nm at incident light intensity of 10 W•m^{-2}.

specific coefficients. For this purpose, Fig. 3(a) – (d) present the specific extinction, absorption, and scattering coefficients obtained from the empirical method, and asymmetry factor determined through the Monte Carlo method, respectively, across light intensities of 10 W•m^{-2}, 20 W•m^{-2}, 40 W•m^{-2}, and 60 W•m^{-2} in the spectral range of 300 nm – 1100 nm.

Fig. 3(b) highlights that the absorption peaks in PPB were not constant throughout tests but rather varied depending on different incident light intensities applied. In more detail, higher light intensities led to lower specific extinction and absorption coefficients. Regarding the peaks in the NIR region, a strong downward shift was observed at incident light intensity of 60 W•m^{-2} in the light absorption of PPB (Fig. 3(b)). This could be probably due to the occurrence of photoinhibition phenomena at incident light intensities above 40 W•m^{-2}, as indicated by Shi and Yu [36]. Regarding the specific absorption coefficient measured at wavelengths from 300 nm to 600 nm, a decrease in the light absorption of PPB was noted at incident light intensities of 40 W•m^{-2} and higher. Carotenoids in this wavelength region play a vital role in photoinhibition protection [37]. When photoinhibition occurs, the degradation of carotenoids takes place as defense mechanism [38], leading to lower absorption coefficients from 40 W•m^{-2} onward. Moreover, in a research work conducted by Cerruti et al. [39] under different light intensities up to 350 W•m^{-2}, lower photopigment contents were observed by increasing light intensity. Indeed, under low light conditions, the mass fractions of bacteriochlorophyll and carotenoid were 4.6 and 10 times higher, respectively, than those under high light conditions. This suggests that light intensity could be used as a controlling factor for guiding the photopigment content in PPB when looking at the recovery of these compounds.

As shown in Fig. 3(c), the scattering is not negligible over the spectral

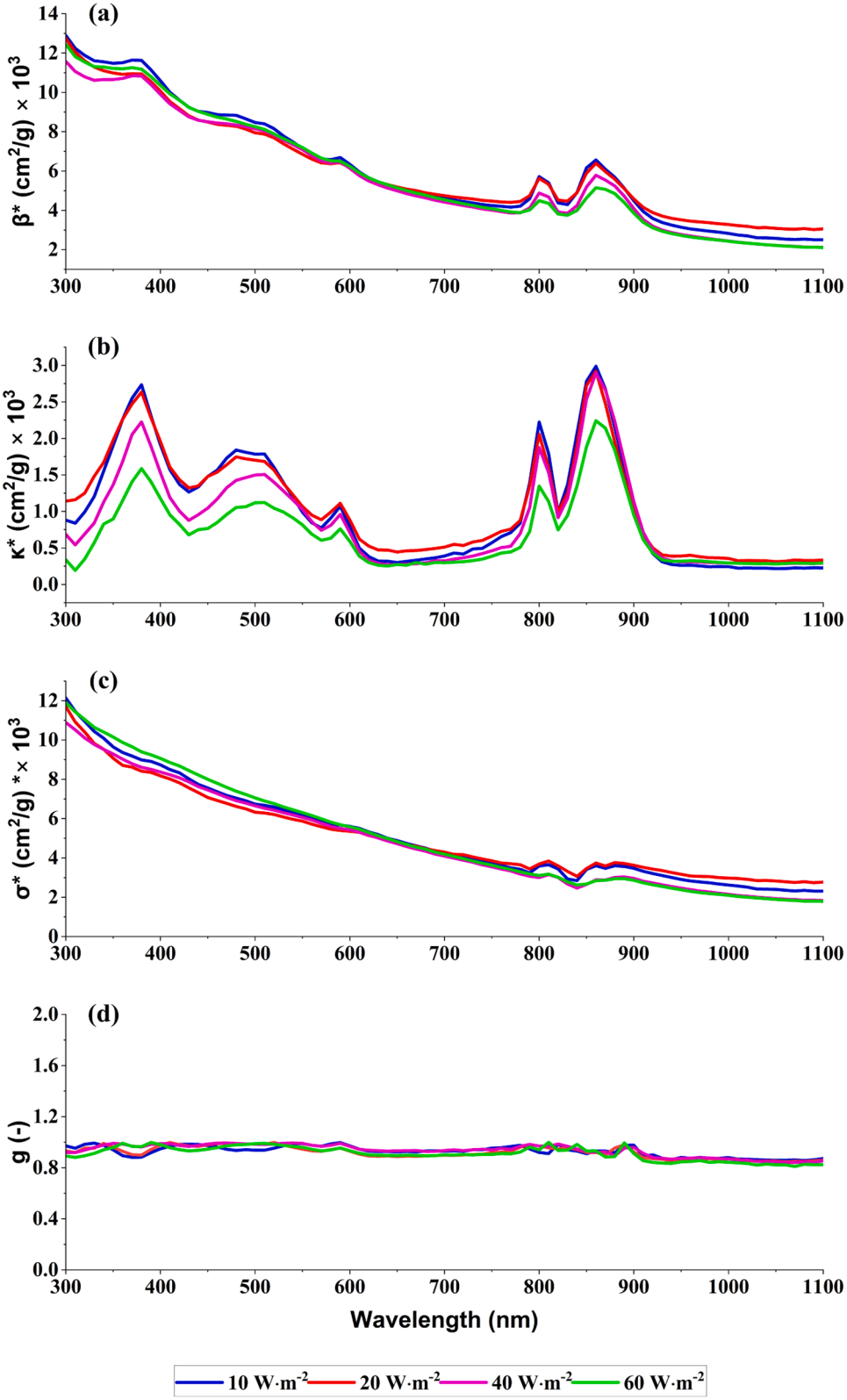

Fig. 3. Specific coefficients of (a) extinction, (b) absorption, (c) scattering, and (d) asymmetry factor (g) for different incident light intensities at wavelengths from 300 nm to 1100 nm.

range from 300 nm to 1100 nm. This result is in line with PPB optical properties measured by Berberoglu and Pilon for a pure culture of PPB [29]. In contrast to absorption, no significant downward trends were observed in scattering by increasing incident light intensities.

Fig. 3(d) illustrates that the asymmetry factor was close to one for all the considered wavelengths at different incident light intensities. These values indicate that forward scattering was the primary occurring phenomenon and confirm the assumptions of Berberoglu and Pilon [29], in which forward scattering prevailed. In more detail, the asymmetry factor equals 0.9 at $\lambda = 850$ nm. The strongly scattered behavior of PPB

is comparable with that of other photosynthetic microorganisms, such as microalgae [40].

As mentioned earlier, the specific coefficients are independent of PPB concentrations. Therefore, the extinction, absorption, and scattering coefficients for any known concentration can be easily obtained. To further investigate the variation in optical properties of PPB under different incident light intensities at a wavelength of 850 nm, β^*_{850}, κ^*_{850}, and σ^*_{850}, are reported in Table 1. Although this is the first measurement of radiation characteristics for PPB mixed cultures under different incident light intensity conditions and there are no literature values for directly comparing the results, the obtained values seem to be higher compared to previous work experimentally measured the optical properties for a pure culture of PPB [29]. This can probably be attributed to the significant differences in the microbial community and operating conditions for the reference study, i.e. a pure culture of PPB grown by applying incident light intensity of 2000 lux – 3000 lux (16 W•m^{-2} – 24 W•m^{-2}) provided by a tungsten light bulb.

3.3. Radiation transfer modelling

To obtain the light intensity profiles for various PPB concentrations at different incident light intensity and biomass concentration conditions, various modelling approaches considered in this study were applied. For the Beer-Lambert law, as previously discussed, Eq. 5 was used to estimate the attenuation profiles based on the estimated extinction coefficients and concentrations at different incident light intensities. Meanwhile, for the two-flux approximation model, curve fitting to experimental data at different incident light intensities was applied and the specific coefficients for absorption (E_a) and scattering (E_s) were estimated, as shown in Table 2.

The two-flux approximation model showed high goodness-of-fit with respect to experimental data, resulting in a difference of values below 1 % in most cases and always less than 5 % (data not shown). The specific absorption and scattering coefficients obtained using this model were higher than the ones experimentally determined in this study (see Section 3.2). This could be attributed to the simplified assumptions considered in this model for two parameters related to light absorption and scattering to effectively describe experimental data depending on the hypothesis of isotropic scattering. However, the estimated values for E_a were within the range of 0.335 – 20 m^2•g^{-1} reported in the previous research works [10,13], and the estimated values for E_s were comparable to the value obtained by Ross and Pott [13]. Moreover, the effect of different incident light intensities on the estimated values by this model was evident, showing that higher incident light intensities led to lower coefficients as observed in optical properties measurements.

For CFD simulations, the experimentally estimated values of radiation characteristics were utilized to obtain the light attenuation profiles at different incident light intensity and biomass concentration conditions. Fig. 4(a) – (d) show attenuation profiles determined by these three models for incident light intensity of 10 W•m^{-2} at different biomass concentrations. It should be noted that to validate the CFD model, a set of simulations was performed using only extinction coefficients as input parameters. By considering these coefficients, the accuracy of CFD model in predicting light attenuation was tested against the Beer-Lambert law. The results demonstrated that the CFD model could replicate the Beer-Lambert law, confirming its reliability in capturing light absorption behaviors based on extinction coefficients (data not shown).

Table 1
Specific extinction, absorption, and scattering coefficients for different incident light intensities at λ = 850 nm determined via empirical method.

I (W•m^{-2})	β^*_{850} (m^2•g^{-1})	κ^*_{850} (m^2•g^{-1})	σ^*_{850} (m^2•g^{-1})
10	0.6180	0.2780	0.3400
20	0.5941	0.2558	0.3383
40	0.5187	0.2536	0.2651
60	0.4531	0.1884	0.2647

Table 2
Specific absorption and scattering coefficients for different incident light intensities at λ = 850 nm determined via two-flux approximation model regression of experimental data.

I (W•m^{-2})	E_a (m^2•g^{-1})	E_s (m^2•g^{-1})
10	0.3960	0.3972
20	0.3763	0.3902
40	0.3482	0.3620
60	0.3216	0.3427

As shown in Fig. 4(a) – (d), all three different models had the same trend in estimating light attenuation profiles throughout the flasks at different biomass concentrations. The light was slightly less attenuated for the two-flux approximation model and CFD simulations compared to the Beer-Lambert law for lower concentrations (Fig. 4(a) and (b)). However, as biomass concentration increased, this difference became negligible (Fig. 4(c) and (d)), indicating that the Beer-Lambert law and the two-flux approximation model could effectively predict the light attenuations inside the PBR. The observed trends highlight that due to the complex RTE solved by CFD simulations, resulting in high computational costs, the use of the Beer-Lambert law as the simplest and easiest modelling approach is a good option for estimating radiation transfer for PPB. This is consistent with the findings of Capson-Tojo et al. [10], suggesting that the Beer-Lambert law was effective in predicting light attenuation. In addition, as light penetrated the PBR containing a PPB suspension, there was a decrease in the light intensity with increasing the light path, which was due to the light absorption and shading effect of the culture. For concentrations lower than 160 mgTSS•L^{-1} (Fig. 4(a) – (c)), the entire reactor was illuminated, while for concentrations higher than 320 mgTSS•L^{-1}, approximately half of the reactor received an almost null amount of light. The same results were observed for the other incident light intensities at different concentrations (shown in Figures S6 – S8 in Supplementary Material). It should be noted that by increasing incident light intensities from 10 W•m^{-2} to 60 W•m^{-2}, the amount of light that reached the deepest part of the reactor at concentrations of 320 mgTSS•L^{-1} was higher (Fig. 4(d), S5 (d), S6 (d), and S7 (d)). As an additional element showing the light distribution in the flasks, the contour plots of light intensity obtained from CFD simulation for incident light intensity of 10 W•m^{-2} are shown in Figures S9 (a) – (d) of Supplementary Material.

These results suggest the importance of proper design of PBRs for ensuring that light penetrates deeply enough to reach all bacterial cells, especially in dense cultures. In addition, selecting a proper light intensity to optimize light distribution throughout the reactor volume is essential for efficient biomass growth and preventing the formation of dark zones where bacteria might not receive sufficient light. Based on the results obtained in this study, the maximum light penetration path with monochromatic light at 850 nm from one side was below 4 cm. This suggests that raceway ponds used for microalgae with a depth of 20 cm – 30 cm are not suitable applications for PPB-based biotechnologies, as light would not reach these depths. This is in line with the results of Capson-Tojo et al. [10], as the study tested the effect of PBR configuration on light attenuation using polychromatic light intensities in the range of 600 W•m^{-2} to 800 W•m^{-2} and concluded the maximum depth for a PPB raceway pond should be below 5 cm. In contrast, flat-plate PBRs are ideal for light-dependent processes due to their thin culture layer and large surface area, which ensure maximized light penetration and uniform light distribution compared to other PBR configurations, such as tubular or cylindrical reactors. However, it is important to note that while a shallower depth may allow for higher light availability and cell density, the overall production might be limited due to the reduced culture volume. To increase the overall production and overcome the formation of dark zones for high PPB

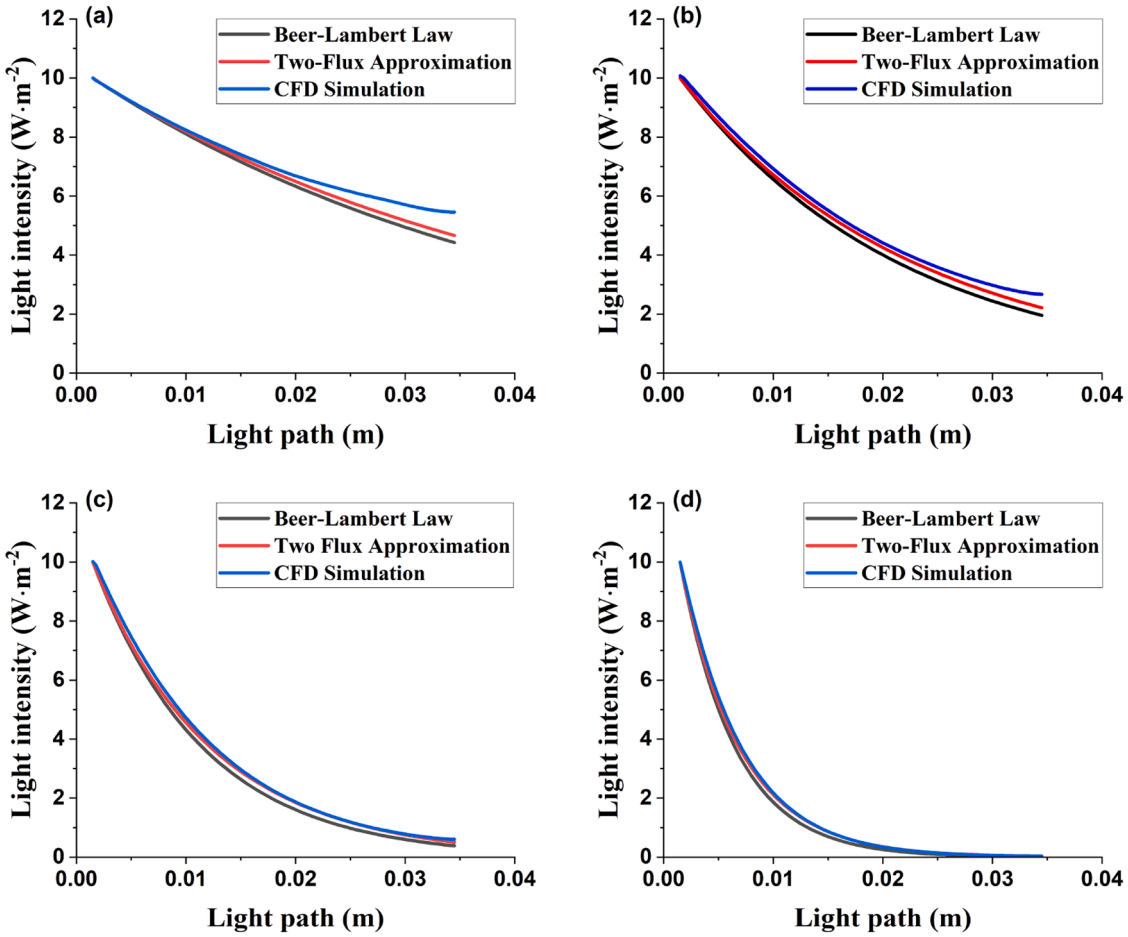

Fig. 4. Light attenuation profiles obtained from the Beer-Lambert law, the two-flux approximation model, and CFD simulations at incident light intensity of 10 W•m^{-2} and different PPB concentrations of (a) 40 mgTSS•L^{-1}, (b) 80 mgTSS•L^{-1}, (c) 160 mgTSS•L^{-1}, and (d) 320 mgTSS•L^{-1}.

concentrations in flat-plate PBRs for having a deeper light path, light can be applied from both sides, potentially allowing for a maximum light penetration path of approximately 10 cm.

To have a better understanding of the average light available throughout the experiments, Fig. 5(a) – (d) compare the average light intensity obtained by the applied models, evidencing higher values for CFD simulations in most cases. This is due to the complex RTE solved by CFD that precisely considered all the phenomena (absorption and scattering) occurring in the PPB suspensions. In particular, it was observed that as PPB biomass concentrations increased, the difference between each model (specifically the Beer-Lambert law and the two-flux approximation model) and CFD simulations results increased in most cases, with the percentage difference values within the range of 0.15 % – 17 % (data not shown). These results suggest that neglecting scattering effect and using Beer-Lambert law for its simplicity, as suggested elsewhere, can lead to slightly lower values for the average light intensity, hence determining errors when applying such values for model parameter estimation.

3.4. *Perspectives on biochemical kinetic modelling*

Although the estimation of biochemical kinetic parameters is beyond the scope of this study, it is crucial to emphasize the importance of identifying the proper approach to include light intensity in kinetic models to accurately represent PPB growth. One approach is to consider the light intensity at the reactor wall or at the raceway top surface as a constant model input value, as it has been done by Puyol et al. [41]. However, although this approach resulted in a good fitting of the experimental data for parameter estimation, it is not realistic as light strongly attenuates crossing the PPB suspension due to a combination of optical phenomena, as it was clearly observed also in the present research work. To address this issue, simple models such as the Beer-Lambert law can be integrated in the biochemical kinetic modelling to describe the light attenuation by applying the average light intensity value for parametric estimation, as reported in Capson-Tojo et al. [42]. This approach is more realistic as the light attenuation is considered. However, the description of the irradiation conditions along the PBR thickness is needed to account for photoinhibition phenomena, thus highlighting the importance of integrating the light attenuation model inside the biochemical kinetic model.

In addition to this, the direct use of light intensity as an input in biochemical kinetic models, being a common practice in most modelling applications on phototrophic microorganisms, is possibly critical in case of highly scattering systems. In particular, the biochemical kinetics for PPB growth depend on the actual fraction of energy that is absorbed by photosystems, which is not proportional to the incident light intensity when scattering is non-negligible. In fact, the absorbed energy differs in principle from computed light intensity at each PBR location and is more effectively described by the LVRPA. Fig. 6(a) – (d) show the LVRPA as a function of the PBR thickness for incident light intensity of 10 W•m^{-2} and different biomass concentrations. Such results enable the computation, and thus the comparison, of the absorbed energy predicted by applying each radiation transfer model. As can be seen, the absorption of photons inside the PPB suspension is not uniform, and not all the layers within the reactor contribute equally to PPB growth, as their productivity depends on the availability of local photons. As expected, the

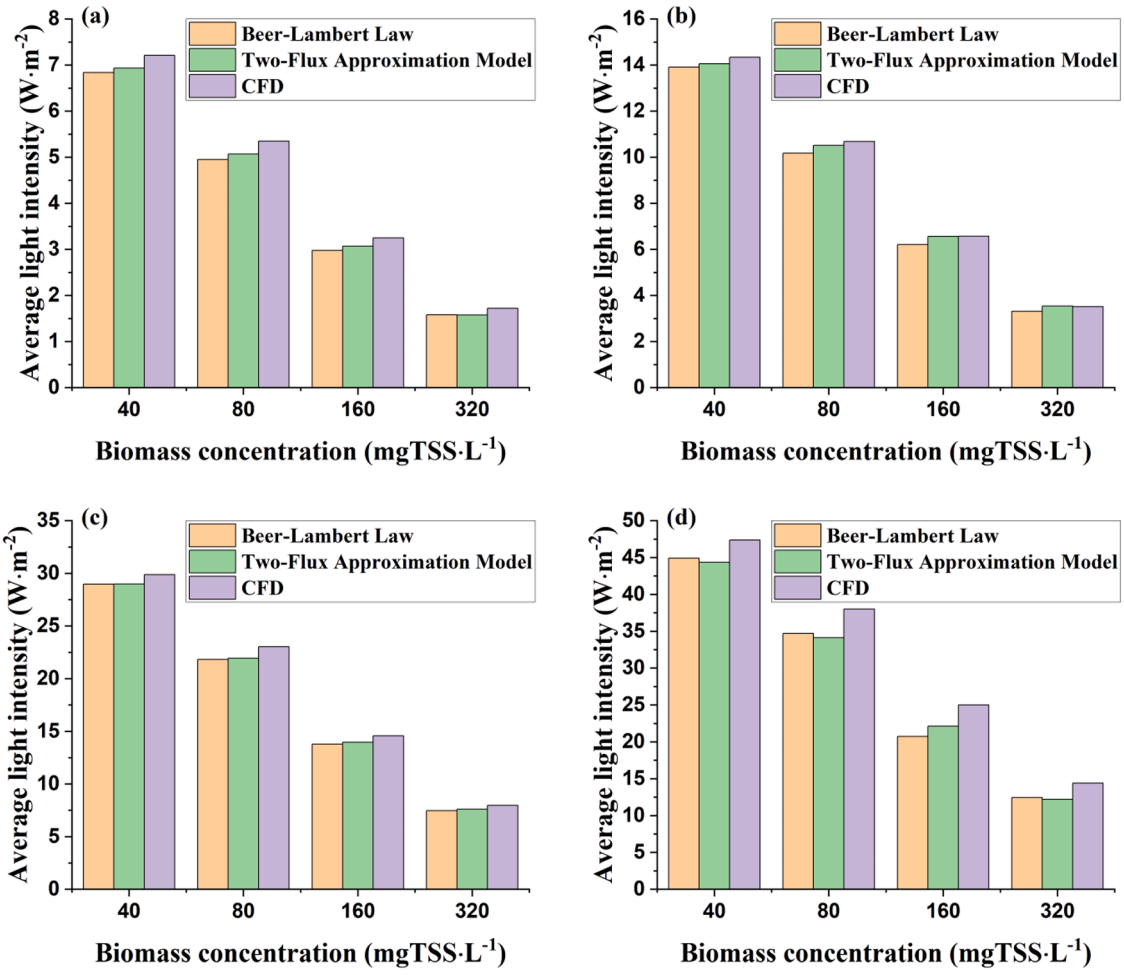

Fig. 5. Average light intensities obtained from the Beer-Lambert law and the two-flux approximation model at different biomass concentrations and incident light intensities of (a) 10 W•m^{-2}, (b) 20 W•m^{-2}, (c) 40 W•m^{-2}, and (d) 60 W•m^{-2}.

LVRPA values obtained from the Beer-Lambert law are higher compared to the other models. This is attributed to the fact that the Beer-Lambert law aggregates the absorption and scattering phenomena as a single value, while the other two models account for absorption and scattering effects separately, resulting in lower values. However, as biomass concentrations increased, the difference between these models decreased.

These results highlighted that the Beer-Lambert law, although effective in describing the light attenuation profile, can lead to errors in calculating the energy absorbed by each layer inside the PBR at lower concentrations. Nonetheless, given that PPB-based biotechnologies often have biomass concentrations higher than 1 gCOD•L^{-1} [4], the difference between this model and CFD simulations could be less pronounced. The same can be stated for the two-flux approximation model although resulting in much more limited differences with respect to CFD simulations, thanks to the empirical inclusion of scattering phenomena in the computation. Therefore, a possible negative outcome of the application of simplified radiation transfer models for integrating light intensity into biochemical kinetic models is the case-specific nature of estimated parameters, as the outputs obtained in the calibration procedure, although successful, could be conditioned by the specific setup geometry or optical characteristics of the liquid medium. Such hypothesis is in agreement with observations reported by Capson-Tojo et al. [10]. The integration of scattering-aware radiation transfer models into LVRPA-based biochemical kinetic models, as is commonly done for other photochemical processes (i.e., photocatalysis) would represent an effective solution to this problem.

Finally, Fig. 6(a) and (b) illustrate that for low biomass concentrations, photons are absorbed along the entire light path of the PBRs, while for higher biomass concentrations, a large portion of incident photons are absorbed in layers closer to the irradiated boundary, with approximately half of the PBR not absorbing enough light energy (Fig. 6(c) and (d)). This is a further demonstration that PPB biomass concentration plays a crucial role in affecting the biochemical process by influencing photon absorption rates. Similar trends were observed for other incident light intensities considered in this study (see Figures S10 – S12 in Supplementary Material). Again, these observations strengthen the importance of adopting a multi-layer modelling approach based on the actual absorbed energy at each PBR location.

4. Conclusions

This study investigated the optical properties of a mixed culture of PPB and assessed the radiation transfer in a flat-plate PBR using the most relevant models and comparing them with CFD simulations in a controlled setup at different incident light intensities ranging from 10 W•m^{-2} to 60 W•m^{-2} and various PPB biomass concentrations. The optical properties obtained by the empirical and Monte Carlo methods yielded roughly equal results over the entire spectral range of wavelengths from 300 nm to 1100 nm. PPB grown with a light intensity of 60 W•m^{-2} showed the lowest specific absorption values at the peaks over the entire spectral range of interest. The results showed that scattering was significant in the mixed culture of PPB, with an asymmetry factor of 0.9 for all the experiments at a wavelength of 850 nm, indicating forward scattering as the prevailing phenomenon. When

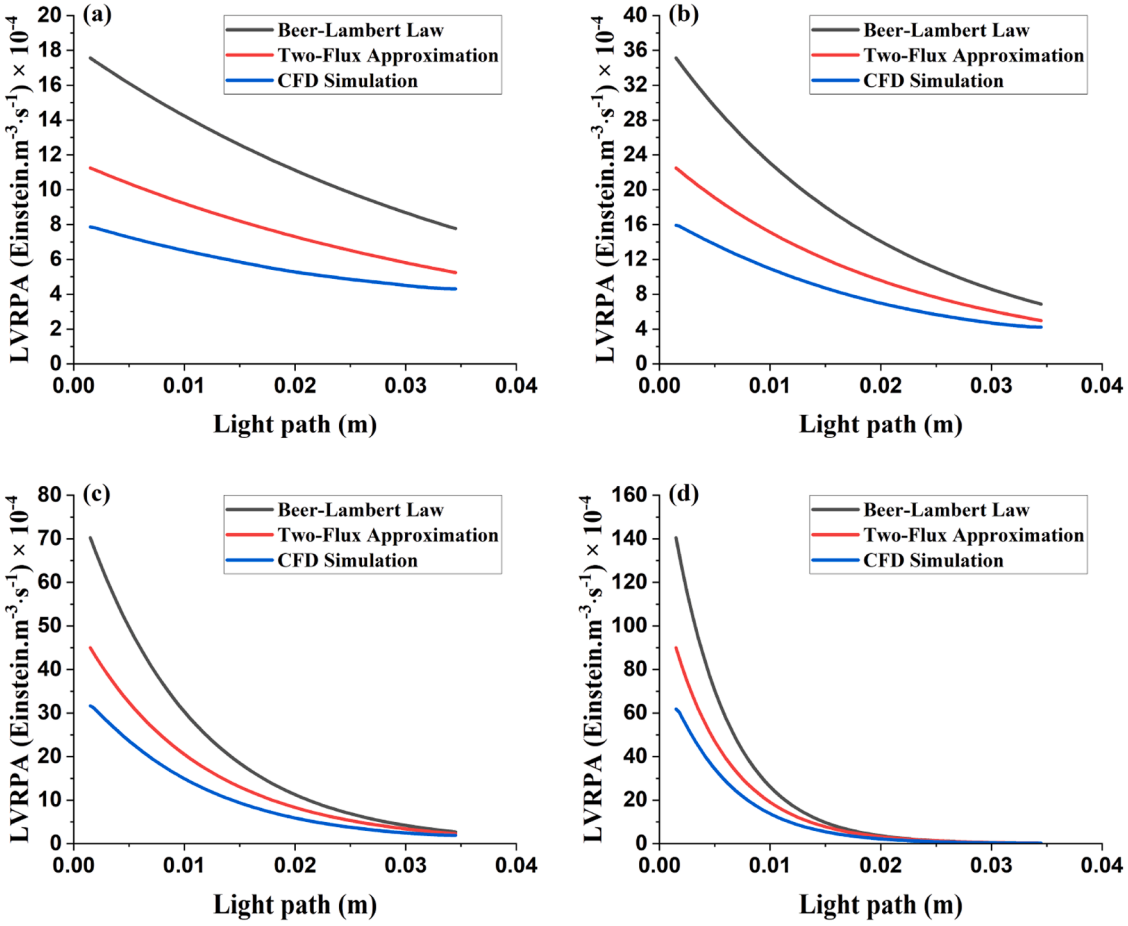

Fig. 6. LVRPA distribution along the light path at incident light intensity of 10 W•m^{-2} and concentrations of (a) 40 mgTSS•L^{-1}, (b) 80 mgTSS•L^{-1}, (c) 160 mgTSS•L^{-1}, and (d) 320 mgTSS•L^{-1} determined by different modelling approaches.

compared with the two-flux approximation model and CFD simulations, the Beer-Lambert law was effective in describing radiation transfer although it led to an overestimation of the LVRPA at lower concentrations, as this model does not differentiate between absorption and scattering phenomena. The maximum light penetration using a light source from one side was found to be less than 4 cm. Consequently, flat-plate PBRs emerged to be more effective for PPB-based biotechnologies rather than raceway ponds since light can be provided from both sides, reducing the formation of dark zones at larger depths. In conclusion, this paper paves the way for selecting and applying appropriate models for the integrated description of radiation transfer and biochemical kinetics in PBR in the view of process scale-up. Further future research activities should focus on understanding the influence of the optical properties of the liquid medium and on extending the assessment to solar energy.

CRediT authorship contribution statement

Ali Amini: Writing – original draft, Visualization, Validation, Software, Methodology, Investigation, Formal analysis, Data curation, Conceptualization. **Elisa Porciatti:** Validation, Software, Methodology, Investigation, Formal analysis, Data curation. **Alessandro Minotto:** Writing – review & editing, Validation. **Álvaro Tolosana Moranchel:** Writing – review & editing, Validation, Software. **Adele Sassella:** Writing – review & editing, Validation, Funding acquisition. **Roberto Canziani:** Writing – review & editing, Validation. **Andrea Turolla:** Writing – review & editing, Validation, Supervision, Resources, Project administration, Methodology, Funding acquisition, Formal analysis, Conceptualization.

Declaration of Competing Interest

The authors declare the following financial interests/personal relationships which may be considered as potential competing interests: Andrea Turolla reports financial support was provided by Italian Ministry of University and Research. Andrea Turolla reports was provided by European Union. Alvaro Tolosana Moranchel reports was provided by Community of Madrid. If there are other authors, they declare that they have no known competing financial interests or personal relationships that could have appeared to influence the work reported in this paper.

Acknowledgements

The research work was partially funded by the PRIN 2022 “PHARPLE” project (ID 2022MHBMEH) funded by the Italian MUR, and the Agritech National Research Center (Task 8.3.2) funded by the European Union Next-GenerationEU (PIANO NAZIONALE DI RIPRESA E RESILIENZA (PNRR) – MISSIONE 4 COMPONENTE 2, INVESTIMENTO 1.4 – D.D. 1032 17/06/2022, CN00000022). The authors would like to gratefully thank the COST ACTION “PURPLEGAIN” (CA21146) funded by the European Union for the training and networking resources made available to the research group, and Dr Luisa Raimondo (Department of Materials Science, University of Milano-Bicocca) for her valuable help in setting up the diffuse reflectance and transmittance spectroscopy experiments. Álvaro Tolosana Moranchel thanks the Consejería de Educación, Juventud y Deporte of the Comunidad de Madrid for the Ayuda Destinada a la Atracción de Talento Investigador “César Nombela” (2023-T1/ECO-29095).

Appendix A. Supporting information

Supplementary data associated with this article can be found in the online version at doi:10.1016/j.jece.2025.115425.

Data Availability

Data will be made available on request.

References

[1] H. Lu, G. Zhang, S. He, R. Zhao, D. Zhu, Purple non-sulfur bacteria technology: a promising and potential approach for wastewater treatment and bioresources recovery, World J. Microbiol. Biotechnol. 37 (2021), https://doi.org/10.1007/S11274-021-03133-Z.

[2] T. Hülsen, K. Hsieh, Y. Lu, S. Tait, D.J. Batstone, Simultaneous treatment and single cell protein production from agri-industrial wastewaters using purple phototrophic bacteria or microalgae – a comparison, Bioresour. Technol. 254 (2018) 214–223, https://doi.org/10.1016/J.BIORTECH.2018.01.032.

[3] F. Meng, A. Yang, G. Zhang, H. Wang, Effects of dissolved oxygen concentration on photosynthetic bacteria wastewater treatment: pollutants removal, cell growth and pigments production, Bioresour. Technol. 241 (2017) 993–997, https://doi.org/10.1016/J.BIORTECH.2017.05.183.

[4] G. Capson-Tojo, D.J. Batstone, M. Grassino, S.E. Vlaeminck, D. Puyol, W. Verstraete, R. Kleerebezem, A. Oehmen, A. Ghimire, I. Pikaar, J.M. Lema, T. Hülsen, Purple phototrophic bacteria for resource recovery: challenges and opportunities, Biotechnol. Adv. 43 (2020) 107567, https://doi.org/10.1016/J.BIOTECHADV.2020.107567.

[5] R. Seto, S. Takaichi, T. Kurihara, R. Kishi, M. Honda, S. Takenaka, Y. Tsukatani, M. T. Madigan, Z.-Y. Wang-Otomo, Y. Kimura, Lycopene-family carotenoids confer thermostability on photocomplexes from a new thermophilic purple bacterium, in: ACS PublicationsR Seto, S Takaichi, T Kurihara, R Kishi, M Honda, S Takenaka, Y Tsukatani, MT MadiganBiochemistry, 14, ACS Publications, 2020, p. 45, https://doi.org/10.1021/acs.biochem.0c00192.

[6] R.G. Saer, R.E. Blankenship, Light harvesting in phototrophic bacteria: structure and function, Biochem. J. 474 (2017) 2107–2131, https://doi.org/10.1042/BCJ20160753.

[7] A.P. Carvalho, S.O. Silva, J.M. Baptista, F.X. Malcata, Light requirements in microalgal photobioreactors: an overview of biophotonic aspects, Appl. Microbiol Biotechnol. 89 (2011) 1275–1288, https://doi.org/10.1007/S00253-010-3047-8.

[8] T. Katsuda, N. Fujii, N. Takata, H. Ooshima, S. Katoh, Light attenuation in suspension of the purple bacterium rhodobacter capsulatus and the green alga chlamydomonas reinhardtii, J. Chem. Eng. Jpn. 35 (2002) 428–435, https://doi.org/10.1252/JCEJ.35.428.

[9] I.S. Suh, S.B. Lee, A light distribution model for an internally radiating photobioreactor, Biotechnol. Bioeng. 82 (2003) 180–189, https://doi.org/10.1002/BIT.10558.

[10] G. Capson-Tojo, D.J. Batstone, M. Grassino, T. Hülsen, Light attenuation in enriched purple phototrophic bacteria cultures: implications for modelling and reactor design, Water Res 219 (2022) 118572, https://doi.org/10.1016/J.WATRES.2022.118572.

[11] G. Naderi, H. Znad, M.O. Tade, Investigating and modelling of light intensity distribution inside algal photobioreactor, Chem. Eng. Process. Process.Intensif. 122 (2017) 530–537, https://doi.org/10.1016/J.CEP.2017.04.014.

[12] J.F. Cornet, C.G. Dussap, G. Dubertret, A structured model for simulation of cultures of the cyanobacterium Spirulina platensis in photobioreactors: I. Coupling between light transfer and growth kinetics, Biotechnol. Bioeng. 40 (1992) 817–825, https://doi.org/10.1002/BIT.260400709.

[13] B.S. Ross, | Robert, W.M. Pott, R.W.M. Pott, Investigating and modeling the effect of light intensity on Rhodopseudomonas palustris growth, Biotechnol. Bioeng. 119 (2022) 907–921, https://doi.org/10.1002/BIT.28026.

[14] L. Pilon, R.K.-A. in C. Engineering, Interaction between Light and Photosynthetic Microorganisms, Elsevier, 2016, https://doi.org/10.1016/bs.ache.2015.12.002.

[15] L. Pilon, H. Berberoğlu, R. Kandilian, Radiation transfer in photobiological carbon dioxide fixation and fuel production by microalgae, J. Quant. Spectrosc. Radiat. Transf. 112 (2011) 2639–2660, https://doi.org/10.1016/J.JQSRT.2011.07.004.

[16] R.J. Brandi, O.M. Alfano, A.E. Cassano, Evaluation of radiation absorption in slurry photocatalytic reactors. 1. Assessment of methods in use and new proposal, Environ. Sci. Technol. 34 (2000) 2623–2630, https://doi.org/10.1021/es9909428.

[17] L. Pilon, H. Berberoğlu, R. Kandilian, Radiation transfer in photobiological carbon dioxide fixation and fuel production by microalgae, J. Quant. Spectrosc. Radiat. Transf. 112 (2011) 2639–2660, https://doi.org/10.1016/J.JQSRT.2011.07.004.

[18] Y.S. Yun, J.M. Park, Attenuation of monochromatic and polychromatic lights in Chlorella vulgaris suspensions, Appl. Microbiol. Biotechnol. 6 (55) (2001) 765–770, https://doi.org/10.1007/S002530100639.

[19] A. Ruiz-Martínez, J. Serralta, A. Seco, J. Ferrer, Modeling light and temperature influence on ammonium removal by Scenedesmus sp. under outdoor conditions, Water Sci. Technol. 74 (2016) 1964–1970, https://doi.org/10.2166/WST.2016.383.

[20] J.M. Heinrich, I. Niizawa, F.A. Botta, A.R. Trombert, H.A. Irazoqui, Analysis and design of photobioreactors for microalgae production II: experimental validation of a radiation field simulator based on a Monte Carlo algorithm, Photochem. Photobio. 88 (2012) 952–960, https://doi.org/10.1111/J.1751-1097.2012.01149.X.

[21] J.-F. Cornet, C.G. Dussap, J.-B. Gros, C. Binois, C. Lasseur, A simplified monodimensional approach for modeling coupling between radiant light transfer and growth kinetics in photobioreactors, Chem. Eng. Sci. 50 (1995) 1489–1500, https://doi.org/10.1016/0009-2509(95)00022-W.

[22] A. Schuster, Radiation through a foggy atmosphere, Astrophys J. (1905).

[23] J. Huang, S. Kang, M. Wan, Y. Li, X. Qu, F. Feng, J. Wang, W. Wang, G. Shen, W. Li, Numerical and experimental study on the performance of flat-plate photobioreactors with different inner structures for microalgae cultivation, J. Appl. Phycol. 27 (2015) 49–58, https://doi.org/10.1007/S10811-014-0281-Y.

[24] P.J. Valadés-Pelayo, F. Guayaquil Sosa, B. Serrano, H. de Lasa, Photocatalytic reactor under different external irradiance conditions: validation of a fully predictive radiation absorption model, Chem. Eng. Sci. 126 (2015) 42–54, https://doi.org/10.1016/J.CES.2014.12.003.

[25] B.A. Cho, R.W.M.C. Pott, The development of a thermosiphon photobioreactor and analysis using computational fluid dynamics (CFD), Chem. Eng. J. 363 (2019) 141–154, https://doi.org/10.1016/J.CEJ.2019.01.104.

[26] J.G. Ormerod, K.S. Ormerod, H. Gest, Light-dependent utilization of organic compounds and photoproduction of molecular hydrogen by photosynthetic bacteria; relationships with nitrogen metabolism, Arch. Biochem Biophys. 94 (1961) 449–463, https://doi.org/10.1016/0003-9861(61)90073-X.

[27] W.D. Collins, J.M. Lee-Taylor, D.P. Edwards, G.L. Francis, Effects of increased near-infrared absorption by water vapor on the climate system, J. Geophys. Res. Atmos. 111 (2006), https://doi.org/10.1029/2005JD006796.

[28] E. Damergi, P. Qin, S. Sharma, M.K. Nazeeruddin, C. Ludwig, Enhancing algae biomass production by using dye-sensitized solar cells as filters, ACS Sustain. Chem. Eng. 9 (2021) 14353–14364, https://doi.org/10.1021/acssuschemeng.1c03780.

[29] H. Berberoglu, L. Pilon, Experimental measurements of the radiation characteristics of Anabaena variabilis ATCC 29413-U and Rhodobacter sphaeroides ATCC 49419, Int J. Hydrog. Energy 32 (2007) 4772–4785, https://doi.org/10.1016/J.IJHYDENE.2007.08.018.

[30] APHA, Standards Methods for the Examination of Water and Wastewater, American Public Health Association, Washington, D.C, 1998.

[31] Á. Tolosana-Moranchel, A. Manassero, M.L. Satuf, O.M. Alfano, J.A. Casas, A. Bahamonde, Influence of TIO2-rGO optical properties on the photocatalytic activity and efficiency to photodegrade an emerging pollutant, Appl. Catal. B 246 (2019) 1–11, https://doi.org/10.1016/J.APCATB.2019.01.054.

[32] R. Pandey, A. Sahu, V. K. K, P. M, Studies on light intensity distribution inside an open pond photo-bioreactor, Bioprocess Biosyst. Eng. 38 (2015) 1547–1557, https://doi.org/10.1007/s00449-015-1398-3.

[33] T. Hülsen, D.J. Batstone, J. Keller, Phototrophic bacteria for nutrient recovery from domestic wastewater, Water Res. 50 (2014) 18–26, https://doi.org/10.1016/J.WATRES.2013.10.051.

[34] P. Dalaei, G. Bahreini, G. Nakhla, D. Santoro, D. Batstone, T. Hülsen, Municipal wastewater treatment by purple phototropic bacteria at low infrared irradiances using a photo-anaerobic membrane bioreactor, Water Res 173 (2020) 115535, https://doi.org/10.1016/J.WATRES.2020.115535.

[35] M. del R. Rodero, J.A. Magdalena, J.P. Steyer, R. Escudié, G. Capson-Tojo, Potential of enriched phototrophic purple bacteria for H2 bioconversion into single cell protein, Sci. Total Environ. 908 (2024) 168471, https://doi.org/10.1016/J.SCITOTENV.2023.168471.

[36] X.Y. Shi, H.Q. Yu, Response surface analysis on the effect of cell concentration and light intensity on hydrogen production by Rhodopseudomonas capsulata, Process Biochem. 40 (2005) 2475–2481, https://doi.org/10.1016/J.PROCBIO.2004.09.010.

[37] H. Hashimoto, C. Uragami, R.J. Cogdell, Carotenoids and photosynthesis, Subcell. Biochem. 79 (2016) 111–139, https://doi.org/10.1007/978-3-319-39126-7_4.

[38] N.K. Choudhury, R.K. Behera, Photoinhibition of photosynthesis: role of carotenoids in photoprotection of chloroplast constituents, Photosynthetica 4 (39) (2001) 481–488, https://doi.org/10.1023/A:1015647708360.

[39] M. Cerruti, J.-H. Kim, M. Pabst, M.C.M. Van Loosdrecht, D.G. Weissbrodt, Light intensity defines growth and photopigment content of a mixed culture of purple phototrophic bacteria, 2022. https://doi.org/10.3389/fmicb.2022.1014695.

[40] R. Kandilian, B. Jesus, J. Legrand, L. Pilon, J. Pruvost, Light transfer in agar immobilized microalgae cell cultures, J. Quant. Spectrosc. Radiat. Transf. 198 (2017) 81–92, https://doi.org/10.1016/J.JQSRT.2017.04.027.

[41] D. Puyol, E.M. Barry, T. Hülsen, D.J. Batstone, A mechanistic model for anaerobic phototrophs in domestic wastewater applications: photo-anaerobic model (PAnM), Water Res. 116 (2017) 241–253, https://doi.org/10.1016/J.WATRES.2017.03.022.

[42] G. Capson-Tojo, D.J. Batstone, T. Hülsen, Expanding mechanistic models to represent purple phototrophic bacteria enriched cultures growing outdoors, Water Res. 229 (2023) 119401, https://doi.org/10.1016/J.WATRES.2022.119401.